Recurrent Intergrowths in the Topotactic Reduction Process of $LaBaCuCoO_{5.2}$

Luisa Ruiz-González,[a] Khalid Boulahya,[a] Marina Parras,[a] José Alonso,[b] and José M. González-Calbet*[a]

Abstract: A new perovskite-related oxide with the $LaBaCuCoO_{5.2}$ composition has been stabilised. Its structure can be described as formed by the recurrent intergrowth of two alternating blocks of $YBaCuFeO_5$ ($2a_c$, i.e., two-fold perovskite superlattice) and $YBa_2Fe_3O_8$ ($3a_c$) structural types. From the starting material $LaBaCuCoO_{5.2-\delta}$ ($\delta = 0$), the rigorous control of the oxygen content has allowed the stabilisation of three new fivefold perovskite-related superstructures with the compositions $\delta = 0.4$, 0.8 and 1.1, which can also be described as recurrent intergrowths of two blocks showing $2a_c$ and $3a_c$ periodicity. The reduction process takes place through the $3a_c$ periodic blocks, when $0 < \delta < 0.8$. Further oxygen decrease seems to involve the $2a_c$ periodic blocks made up of pyramidal layers, giving rise to infinite layer units. The stability limit for these fivefold superstructures is $\delta = 1.1$. In agreement with this the as-synthesised materials constitute an example of topotactic reaction, since their basic structure is kept through the reduction process.

Keywords: electron diffraction · electron microscopy · intergrowth phases · perovskite phases

Introduction

Cobaltites have been widely studied as they show unique electronic and magnetic properties as a consequence of the ability of Co to adopt II, III and IV oxidation states as well as low-, intermediate- and high-spin states. Moreover, cobalt atoms can exhibit several coordination environments, giving rise to different structures. Among them, perovskite-related cobalt oxides play an important role, since they can easily accommodate compositional variations and, hence, induce changes in the properties. When basic relationships linking properties to crystal structure and chemical compositions are understood new more efficient materials can be developed or performances of known materials can be improved.

The basic $ACoO_3$ stoichiometry can be stabilised in two polytypes, depending on the size of the A cation: 3C (cubic stacking of the AO_3 layers) and 2H (hexagonal stacking of the AO_3 layers). For instance, $LaCoO_3$,[1] although rombohedraly distorted, is related to the cubic perovskite, while Ba^{2+} stabilises the 2H-$BaCoO_3$ polytype.[2] In both cases, oxygen defines octahedral holes in which cobalt atoms are placed. $[CoO_6]_o$ moieties (o stands for octahedral coordination) share corners and faces in the 3C and 2H polytypes, respectively. Reduction of the oxygen content can give rise to new phases as a consequence of ordered rearrangement of the non-occupied oxygen positions. This is indeed possible owing to the cobalt ability to adopt tetrahedral and pyramidal oxygen coordination as well as the, already mentioned, different oxidation states.

We describe in this paper some new oxygen-deficient phases related to the cubic polytype. An interesting example, which combines both promising properties and flexibility to accommodate oxygen vacancies in new ordered patterns, is the case of $LnBaCo_2O_{5+\delta}$ (Ln = Pr, Nd, Sm, Eu, Gd, Tb) compounds.[3] Their great interest is focused on its magnetoresintant behaviour[4] as the better known La-Ca-Mn perovskite system.[5] From the structural point of view, ordering of nonoccupied oxygen positions in $LnBaCo_2O_{5+\delta}$ leads to the formation of square pyramids. In this sense, materials with $\delta = 0$ (3) are built up of square-pyramids that share corners (Figure 1a), and are isostructural to $YBaCuFeO_5$.[6] A higher oxygen content leads to $LnBaCo_2O_{5.5}$,[3] whose structure can

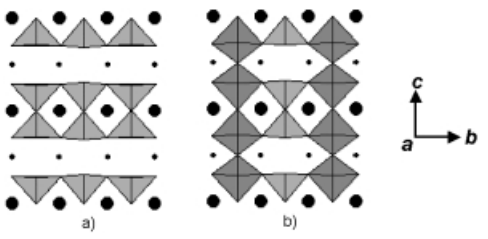

Figure 1. a) Structural model corresponding to $YBaCo_2O_5$, isostructural to $YBaCuFeO_5$. b) Structural model corresponding to $LnBaCo_2O_{5.5}$

[a] Prof. J. M. González-Calbet, Dr. L. Ruiz-González, Dr. K. Boulahya, Dr. M. Parras
Dpto. Química Inorgánica
Facultad de Ciencias Químicas
Universidad Complutense de Madrid, 28040-Madrid (Spain)
Fax: (+34) 91-3944342
E-mail: jgcalbet@quim.ucm.es

[b] Dr. J. Alonso
Instituto de Ciencia de Materiales de Madrid, CSIC
Cantoblanco, 28049 Madrid, Spain

0947-6539/02/0824-5694 $ 20.00+.50/0 *Chem. Eur. J.* **2002**, *8*, No. 24

be described as formed by the ordered intergrowth of octahedra and square pyramids of Co atoms along the *b* direction (Figure 1b). Besides these ordered structures, phases with intermediate oxygen contents, $LnBaCo_2O_{5.3}$ (Ln = Dy, Ho), show areas based on intergrowths of one octahedron and two pyramids with a theoretical stoichiometry of 5.11 oxygen atoms per unit formula, as observed by high-resolution electron microsocpy (HREM).[3]

The above ordered intergrowths were initially described in the oxygen deficient perovskite system $YBaCo_{2-x}Cu_xO_{5+\delta}$[7] when studying the relationship between superconductivity and magnetism in high T_c superconductors. Although up to now undoped cobalt compounds have attracted more attention owing to their transport properties, the Cu-substituted ones can show a broader crystallochemistry. Actually, in addition to the octahedral, square-pyramidal and tetrahedral environments available for cobalt cations, copper can also adopt square-planar and linear coordinations. Therefore, the mixture of both cations, Cu and Co, at the B perovskite positions should open more structural possibilities.

Taking into account the above ideas the aim of this work has been the search of new ordered phases in the $LaBaCuCoO_{5+\delta}$ system. It is worth noticing that Y has been substituted by La; since both cations have different polarizing power,[8] that is, different q/r ratio, their oxygen avidity is not the same and, hence, compositional and structural changes are expected.

Results and Discussion

$LaBaCuCoO_{5.2}$: The X-ray diffraction (XRD) pattern of the starting material, $LaBaCuCoO_{5.2}$, can be indexed on the basis of a cubic perovskite, although slightly broad maxima are observed. To analyse the microstructure of this material selective area electron diffraction (SAED) and HREM studies were performed.

The SAED pattern along $[001]_c$ (Figure 2a) is in agreement with the basic cubic perovskite cell according to the XRD information. Additional weaker reflections, along *b**, are observed in the $[1\bar{1}0]_c$ pattern (Figure 2b). Such reflections

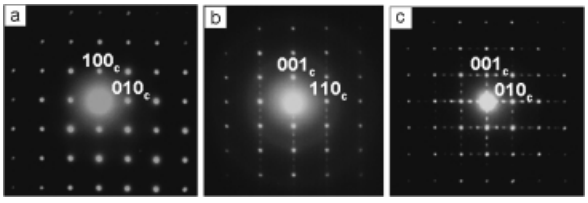

Figure 2. SAED pattern corresponding to $LaBaCuCoO_{5.2}$ along a) $[001]_c$; b) $[1\bar{1}0]_c$ and c) $[100]_c$ zone axes.

seem to be related to the presence of a fivefold superstructure, since they appear at 2/5 and 3/5. Weak streaking along *c* is indicative of some structural disorder which will be further discussed. Figure 2c is an SAED pattern along the $[100]_c$ zone axis, in which superlattice reflections, at 2/5 and 3/5, appear either along *b** and *c** directions. Since superstructure spots along *b* are absent in $[001]_c$ pattern (Figure 2a) they could be related to the presence of perpendicular domains. This is, indeed, a quite usual phenomenon in perovskite-related materials.[11, 12] According to that, a modulated fivefold superlattice along the cubic *c* axis is evident. Besides, it is worth recalling that distances along *a** and *b** are identical (Figure 2a). Therefore, from the SAED results, a tetragonal unit cell $a_c \times a_c \times 5a_c$ can be proposed for $LaBaCuCoO_{5.2}$, in which a_c stands for the cubic perovskite subcell parameter. To confirm the tetragonal symmetry, a microdiffraction study was performed. Patterns along $[100]_c$ and $[001]_c$ are shown in Figure 3a and b, respectivelly, in which mirror planes are observed and superimposed in the figure, suggesting a possible *P*4/*mmm* symmetry.

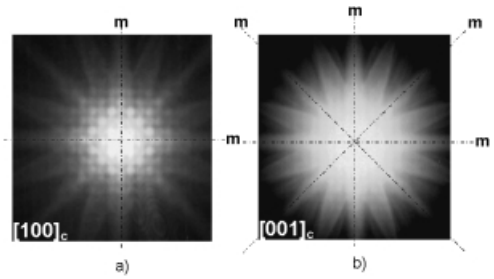

Figure 3. Microdiffraction patterns corresponding to $LaBaCuCoO_{5.2}$ along a) $[100]_c$ and b) $[001]_c$.

Figure 4 is a HREM image along $[100]_c$. The image confirms the existence of perpendicular domains as well as the fivefold order superstructure along *c*. Such a super

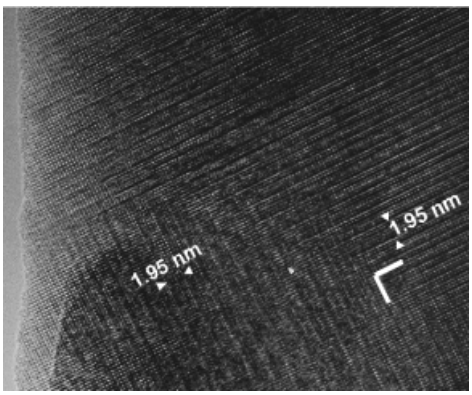

Figure 4. HREM image along $[100]_c$ of $LaBaCuCoO_{5.2}$. Perpendicular domains are apparent.

structure, as better observed in the enlarged image (Figure 5a), is built up of blocks of $2a_c$ and $3a_c$ periodicity (marked on the image). The $2a_c$ periodic unit is made up of bright-dark-bright motifs, while the $3a_c$ incorporates one dark more (bright-dark-dark-bright). Notice the brightest contrast limiting both blocks. As described in the introduction section, ordered stacking of octahedra and square-planar pyramids is characteristic of oxygen deficient cobaltites. According to that, blocks of $3a_c$ and $2a_c$ periodicity could be related to the polyhedra sequence $\cdots PO_hP \cdots$ and $\cdots PP \cdots$, respectively (P = square-pyramid; O_h = octahedron). Those sequences constitute the structural features characteristic of $YBa_2Fe_3O_8$[13] ($\cdots PO_hP \cdots$) and $YBaCuFeO_5$[6] ($\cdots PP \cdots$) structural types (Figure 6a and b, respectively). An ordered

  0947-6539/02/0824-5695 $ 20.00+.50/0

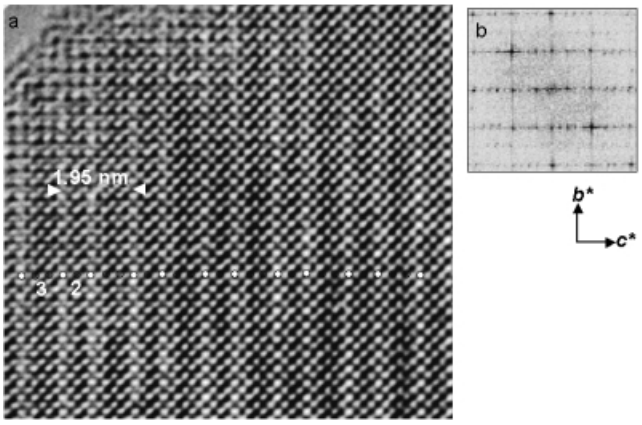

Figure 5. a) Enlarged HREM image of an ordered domain of $LaBaCuCoO_{5.2}$ along $[100]_c$. Blocks of $3a_c$ and $2a_c$ periodicity are marked. b) FT of the above image showing fivefold superstructure.

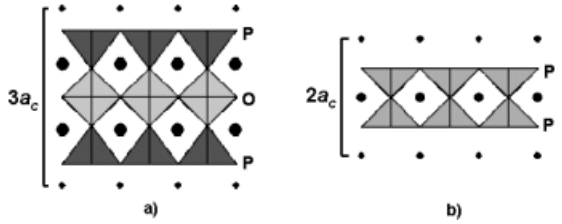

Figure 6. Structural models corresponding to the a) $YBa_2Fe_3O_8$ and b) $YBaCuFeO_5$ types.

arrangement of both units, $\cdots PO_hP\ PP\cdots$, would give rise to a fivefold superstructure and the oxygen content would be in agreement with the experimental one. However, this periodicity seems to be interrupted, in some areas, due to the junction of two blocks of the same periodicity $3a_c$ or $2a_c$, giving rise to a contrast inversion (marked in Figure 7). On the

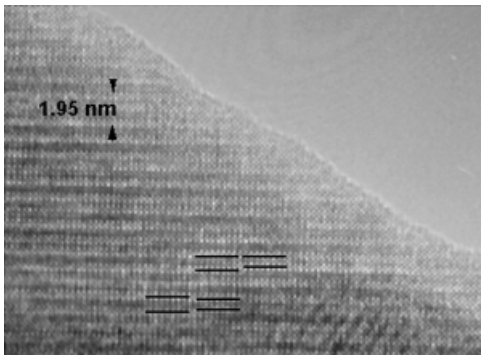

Figure 7. Detail of a HREM image of $LaBaCuCoO_{5.2}$ along $[100]_c$ showing local changes in the $\cdots 3a_c-2a_c\cdots$ sequence.

basis of the polyhedra sequence described above, the differences in contrast observed in the image (Figure 7) could be explained as induced by a change in the metal coordination and/or composition. For instance, it is worth noticing, as schematically represented in Figure 8, that periodicity of a $2a_c$ block can be disturbed if a P pyramidal block is changed to an octahedral one O_h. This nonordered occurrence of O_h and/or P polyhedra would involve a random distribution of the Cu/Co cations. In this sense, as already pointed out, differences in

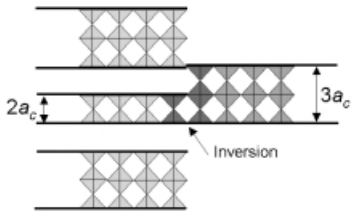

Figure 8. Schematic representation showing local changes in blocks periodicity.

the Cu/Co ratio along the crystal have been detected, being, probably, the cause of the local change of periodicity observed as contrast inversions in the experimental images. The presence of perpendicular domains as well as the local interruption of the ordered $\cdots 2a_c-3a_c\cdots$ sequence, avoids the existence of long-range order. However, the corresponding Fourier transform (FT) (Figure 5 b), in which all superlattice spots appear, evidences fivefold order.

To obtain more reliable structural information, crystallographic image processing (CIP) was performed. The CIP technique, by combining both SAED and HREM information, leads, after corrections, to gather potential maps. In this work, the CRISP program[14] was used for image processing. The steps followed in CIP are represented in Figure 9. Figure 9a corresponds to a thin area of the experimental

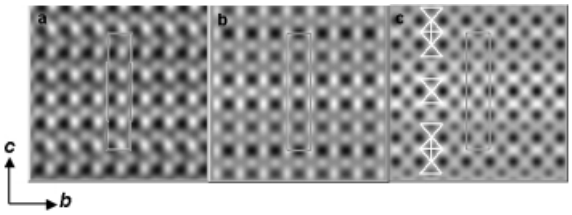

Figure 9. a) Experimental high-resolution image corresponding to $LaBaCuCoO_{5.2}$. b) Processed image. c) Potential map obtained after applying (*pmm*) symmetry. Unit cell and structural model are outlined.

image along $[100]_c$. Figure 9b is a potential map obtained after some corrections, tilt, CTF, phases and amplitudes. After symmetry application (*p2mm*), according to the space group *P4/mmm* determined by SAED and CBED, the final potential map (Figure 9c) is obtained; this confirms the fivefold superstructure. Since no differences in the black contrast (related to the cation positions) are observed, there is no evidence of cation order in a fivefold superstructure. In fact, the cation relation La/Ba/Cu/Co = 1:1:1:1 does not seem to favour such an order. Moreover, Cu and Co order could not be detected by this technique, since both cations have similar atomic numbers. Although it is not possible to determine the oxygen exact position by CIP, differences in white contrasts are observed. It is, in fact, well known that under the optimum defocus conditions the brightest contrast corresponds to the lower potential areas, that is, oxygen and oxygen vacancies. In this sense, the superstructure must be induced by an ordered arrangement of oxygen vacancies in agreement with the polyhedral model previously mentioned (Figure 10a) ($\cdots PO_hP\ PP\cdots$) and superposed on the potential map. Cobalt and copper must be randomly arranged at the B positions of

  0947-6539/02/0824-5696 $ 20.00+.50/0 *Chem. Eur. J.* **2002**, *8*, No. 24

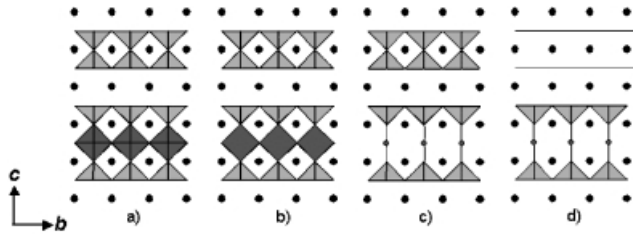

Figure 10. Structural models proposed for a) $LaBaCuCoO_{5.2}$, b) $LaBaCuCoO_{4.8}$, c) $LaBaCuCoO_{4.4}$ and d) $LaBaCuCoO_4$.

the basic ABO_3 perovskite structure, that is, at the octahedral and pyramidal environments.

On the basis of the above results, X-ray profile refinement of $LaBaCuCoO_{5.2}$ was performed taking as starting point the structural model obtained by SAED and HREM. Figure 11 shows the graphic results of the fitting of the experimental

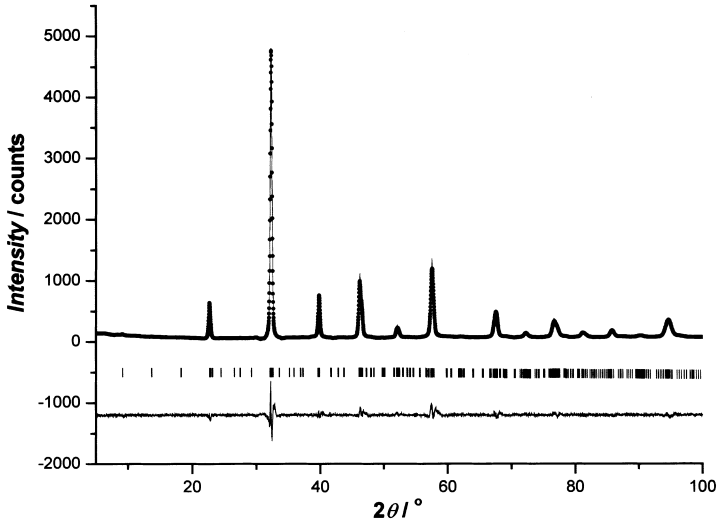

Figure 11. Experimental (points), calculated (solid lines) and difference (bottom) X-ray diffraction patterns for $LaBaCuCoO_{5.2}$.

X-ray diffraction pattern and the difference between observed and calculated data. The final structural parameters are collected in Table 1, whereas some selected interatomic distances are gathered in Table 2. The structural refinement confirms the model obtained by SAED and HREM (Figure 10a). The essential feature of the structure is the presence of a well-ordered intergrowth between PP and PO_hP blocks, that is, basic units of the $YBaCuFeO_5$ and $YBa_2Fe_3O_8$ structural types along the *c* axis, in which La, Ba and Cu, Co atoms are randomly distributed over A and B sites of the $ABO_{2.6}$ lattice, respectively. (La/Ba)1 and (La/Ba)3 are coordinated by twelve oxygen atoms, whilst (La/Ba)2 have eightfold coordination. The obtained values for all (La/Ba)–O distances are reasonable and consistent with previously reported bond lengths in other comparable oxides.[15] (Cu/Co)1 are octahedrally coordinated by nearby oxygen atoms at distances ranging from 1.89–1.96 Å. The (Cu/Co)2 and 3 occupy quite regular square pyramids characterised by four (Cu/Co)–O equatorial equivalent distances (see Table 2). All M–O distances are comparable to those found for Cu or Co in the same oxygen environments.[6, 16]

Table 1. Final structural parameters of $LaBaCuCoO_{5.2}$.[a]

Atom	*x*/*a*	*y*/*b*	*z*/*c*	*B* [Å^2]	Occupancy
Cu/Co1	0	0	0	0.17(8)	1
Cu/Co2	0	0	0.203(1)	0.17(8)	1
Cu/Co3	0	0	0.395(1)	0.17(8)	1
La/Ba1	0.5	0.5	0.1014(6)	0.77(4)	1
La/Ba2	0.5	0.5	0.3010(6)	0.77(4)	1
La/Ba3	0.5	0.5	0.5	0.77(4)	1
O1	0	0	0.097(5)	0.22(3)	1
O2	0	0.5	0.213(2)	0.22(3)	1
O3	0	0.5	0.414(2)	0.22(3)	1
O4	0	0	0.5	0.22(3)	1
O5	0.5	0	0	0.22(3)	1

[a] Space group = *P*4/*mmm* (no. 123), $a = 3.9352(3)$, $c = 19.538(2)$ Å, $R_{wp} = 11.1\,\%$, $R_B = 3.74\,\%$ $R_p = 4.88\,\%$, $\chi^2 = 1.61\,\%$.

Table 2. Selected interatomic distances [Å] in $LaBaCuCoO_{5.2}$.

La/Ba1–O1	2.783(3) × 4	Cu/Co1–O1	1.89(9) × 2
La/Ba1–O2	2.95(3) × 4	Cu/Co1–O5	1.966(1) × 4
La/Ba1–O5	2.79(8) × 4	Cu/Co2–O1	2.07(9)
La/Ba2–O2	2.602(3) × 4	Cu/Co2–O2	1.98(5) × 4
La/Ba2–O3	2.96(3) × 4	Cu/Co3–O3	1.999(9) × 4
La/Ba3–O3	2.58(3) × 8	Cu/Co3–O4	2.03(3)
La/Ba3–O4	2.781(1) × 4		

It is worth recalling, that structural blocks of $3a_c$ periodicity constitute the basic units of different $LnBa_2B_3O_{7+\delta}$ compounds (Ln and B means rare-earth and metal of the first transition-series cations, respectively). Besides the above-mentioned $YBa_2Fe_3O_8$ type,[13] characterised by the polyhedra sequence $\cdots POhP \cdots$, $YBa_2Cu_3O_7$[17] and $YBa_2Cu_3O_6$[18] exhibit similar periodicity,that is, $3a_c$. However, the central polyhedron of these blocks is different to that present in the iron compound as a consequence of the Cu ability to stabilise square-planar and linear oxygen coordination. In this sense, the $YBa_2Cu_3O_7$ structure can be described as built up from the polyhedra squence $\cdots PS_PP \cdots$ (S_P = square-planar coordination), whilst the lower content oxide $YBa_2Cu_3O_6$ shows the $\cdots PLP \cdots$ (L = linear) one. It is then clear that the reduction process $YBa_2Cu_3O_7 \rightarrow YBa_2Cu_3O_6$ involves a change of the copper environment from S_P to L. On the basis of these facts, if Cu, in $LaBaCuCoO_{5.2}$, occupied the octahedral central position of the $\cdots PO_hP \cdots$ block, a similar reduction path would be expected for new $LaBaCuCoO_{5.2-\delta}$ compounds thorough the $3a_c$ periodic block. Since the threefold order should not be drastically affected due to the coordination change ($O_h \rightarrow S_P \rightarrow L$), while the pyramid layer is to be maintained, the fivefold superstructure should be also kept in the "hypothetical" reduction process.

According to this, in order to test the validity of the above proposal, samples of nominal composition $LaBaCuCoO_{4.8}$ and $LaBaCuCoO_{4.4}$, corresponding to the anionic composition required to the formation of S_P and L, respectively, were prepared in an electrobalance, as described in the experimental section.

$LaBaCuCoO_{5.2-\delta}$: XRD patterns of $\delta = 0.4$ and $\delta = 0.8$ samples can be indexed, as the starting material $LaBaCuCoO_{5.2}$, on the basis of a cubic perovskite. Cation compositions are in

agreement to the nominal ones. However, again, EDS analysis indicates that, although in average constant, the Cu/Co ratio changes over small areas.

SAED patterns corresponding to both $LaBaCuCoO_{4.8}$ and $LaBaCuCoO_{4.4}$ oxides along $[1\bar{1}0]_c$ and $[100]_c$ zone axes (Figure 12a, b) are similar to those of the higher oxygen

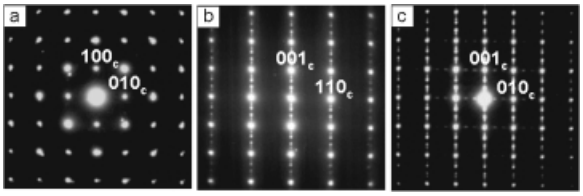

Figure 12. SAED patterns corresponding to $LaBaCuCoO_{4.8}$ along a) $[100]_c$; b) $[1\bar{1}0]_c$ and c) $[001]_c$ zone axes. Identical results are obtained for $LaBaCuCoO_{4.4}$.

content sample; this suggests that the fivefold modulated superlattice is preserved in the reduction. However, in the SAED pattern along $[001]_c$ (Figure 12c) it can be appreciated that a^* and b^* are slightly different, thus indicating a small orthorhombic distortion and $P2/mmm$ as possible space group. HREM study confirms the fivefold superlattice. Actually, 1.95 nm periodicity along c is observed in Figure 13a, which is a HREM image corresponding to the

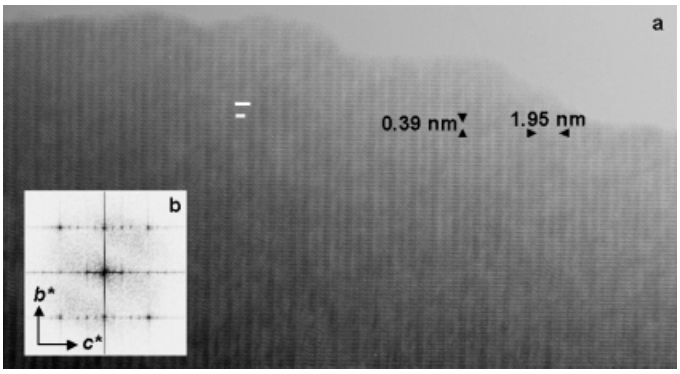

Figure 13. a) HREM image corresponding to $LaBaCuCoO_{4.8}$ along $[100]_c$. b) Corresponding FT.

$LaBaCuCoO_{4.8}$ sample. The corresponding FFT (Figure 13b) shows again the fivefold superstructure. Once again, a CIP study was performed on a thin area of the above image. Figure 14 depicts the potential map obtained after corrections and applying symmetry. As in the starting material, $LaBaCuCoO_{5.2}$, the fivefold order is clearly seen, while, at the same

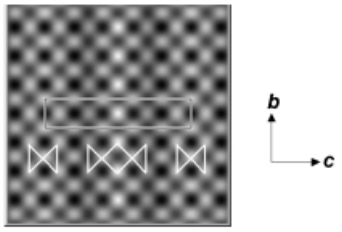

Figure 14. Potential map corresponding to $LaBaCuCoO_{4.8}$. Unit cell and structural model are outlined.

time, there is no evidence of cation ordering. These results would be in agreement with the $\cdots PP\,PS_PP\cdots$ stacking polyhedra sequence proposed for $LaBaCuCoO_{4.8}$ with a random A (La/Ba) and B (Cu/Co) distribution over the corresponding lattice positions with the exception of the square-planar coordination site, which seems logical to be occupied by Cu. On the other hand, as happens in $LaBaCuCoO_{5.2}$, local changes at the $\cdots 2a_c - 3a_c \cdots$ periodicity are observed in the HREM of Figure 13. The origin of such a discontinuity could be again understood on the basis of the small differences in Cu/Co ratio, detected by energy-dispersive spectroscopy (EDS), over small areas. In this case, the periodicity of a $2a_c$ block can be disturbed if a P polyhedron is subtituted by a S_P one, taking into account the Cu ability to adopt either pyramidal or square-planar coordination in oxide compounds.

Although, diffraction data corresponding to the sample with lower oxygen content, $LaBaCuCoO_{4.4}$, are similar to those of $LaBaCuCoO_{4.8}$, CIP shows noticeable differences. Figure 15a corresponds to HREM image along $[100]_c$ and Figure 15b is the corresponding potential map obtained after

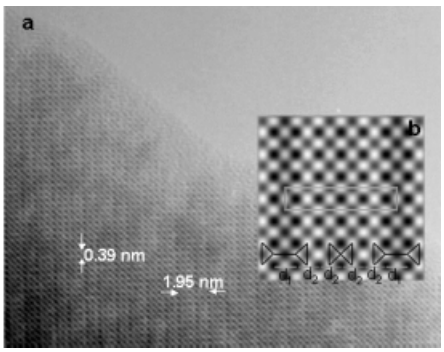

Figure 15. a) HREM image and b) potential map along $[100]_c$ corresponding to $LaBaCuCoO_{4.4}$. The two different distances ($d_1 < d_2$) between the B cations are clearly seen.

CIP was performed. The map shows, in addition to the fivefold superlattice, two different distances (marked on Figure 15b), d_1 and d_2, between the A cations, with $d_1 < d_2$. The shortest distance (d_1) affects to the central position of the $3a_c$ periodic block. At this point, it is worth recalling that La/Ba ionic radius, in accordance to Shannon,[19] decreases when the coordination number is lower. In this sense, the shortest detected distance (d_1) could be related to a lower La/Ba cation coordination in the mentioned block. This would, in fact, involve a reduction of the coordination of the B cation (Cu), placed at the central position of the $3a_c$ periodic block according to $S_P \rightarrow L$.

These structural facts allow to propose not only the stabilisation of three new phases, $LaBaCuCoO_{5.2}$, $LaBaCuCoO_{4.8}$, $LaBaCuCoO_{4.4}$, but also the reduction mechanism of the first one, $LaBaCuCoO_{5.2}$, as represented in Figure 10a–c, through the $3a_c$ periodic blocks. Moreover, although it is not possible to determine by XRD or microscopy the Co/Cu arrangement, the obtained samples only would be stable if copper occupies the central position of the threefold unit. The three oxides are fivefold superstructures of the basic perov-

0947-6539/02/0824-5698 $ 20.00+.50/0 *Chem. Eur. J.* **2002**, *8*, No. 24

skite one and can be described as recurrent intergrowths[20] of two sequences of periodicity $2a_c$ and $3a_c$. The first one, built up of square pyramids, is kept through the reduction process, whereas a decrease in oxygen content seems to be associated to the second one. As a consequence, a new ordered arrangement of the nonoccupied oxygen positions at the starting octahedral site in the $\cdots PO_hP\cdots$ sequence of the $LaBaCuCoO_{5.2}$ is created.

The possibility to stabilise lower oxygen-content samples has been also studied. In this sense, a material with the fivefold superstructure is stable up to 4.1 oxygen atoms per unit formula. XRD and SAED patterns are similar to those corresponding to $\delta = 0.4$ and 0.8 samples. Figure 16 a is a HREM image along $[100]_c$ zone axis. Periodicity of 1.95 nm,

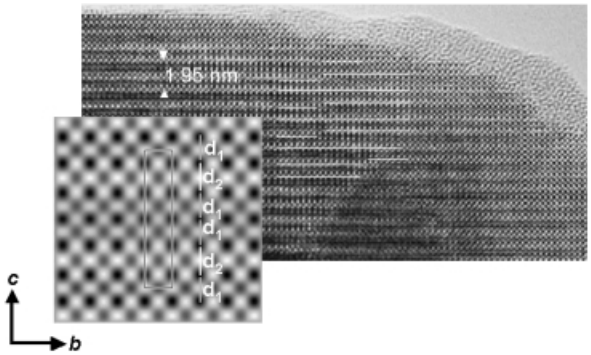

Figure 16. a) HREM image along $[100]_c$ corresponding to $LaBaCuCoO_{4.1}$. Contrast variations due to local changes in block periodicities are outlined. b) Corresponding potential map. The two different distances ($d_1 < d_2$) between the B cations are observed.

that is, $5a_c$, is clearly observed. Compositional analysis is in agreement with the nominal one. However, it is worth pointing out that averaging changes on the Co/Cu ratio, over small areas, are even more remarkable than in more oxidised samples. According to this, the contrast inversion (marked with white lines), described in the above samples, appears more frequently in $LaBaCuCoO_{4.1}$, being related to coordination changes as a consequence of the compositional variation.

CIP was again performed over a thin area of the image. Two different distances can be observed in the potential map (Figure 16b), $d_1 < d_2$, as happens in the $LaBaCuCoO_{4.4}$ sample. Nevertheless, the arrangement of these periodicities is different in both compounds. Such a distribution is $\cdots d_1d_2d_2d_2d_2\cdots$ in $LaBaCuCoO_{4.4}$ and $\cdots d_1d_2d_1d_1d_2\cdots$ in $LaBaCuCoO_{4.1}$. One of the d_1 distances in $LaBaCuCoO_{4.1}$ corresponds to the $3a_c$ periodic block, as in sample $LaBaCuCoO_{4.4}$, in agreement with the linear environment for Cu atoms. The other d_1 distance involves the $2a_c$ unit and, therefore, it could be associated with a lower coordination of the pyramidal layers, that is, a square-planar one, giving rise to an infinite layer unit.[21] A tentative structural model for this sample is shown schematically in Figure 10d. The corresponding oxygen content would be four atoms per unit formula, slightly different from the experimental value (4.1). As we have already mentioned, Cu can easily adopt square-planar coordination, but this is not the case for Co. According to this, it seems that Cu is involved not only in the $3a_c$ unit, but also in the $2a_c$ periodic block and, thus, a Cu/Co ratio 3:2 would result. Therefore, both the Cu/Co ratio and the oxygen content are different from the ideal values. This different composition could be responsible for the local changes in contrast observed in the experimental image and the real model must be built up of randomly areas of different composition, that is, $LaBaCuCoO_{4.4}$ and $LaBaCuCoO_4$. The different kind of possible environments seems to favour random substitution and then local changes in periodicity. In any case, CIP results suggest the existence of square-planar environments in the $LaBaCuCoO_{4.1}$ oxide. This means that reduction of the oxygen content in $LaBaCuCoO_{4.4}$ takes place through the block of $2a_c$ periodicity instead of through the $3a_c$. By the way, this process seems logical, since oxygen elimination on the $3a_c$ blocks $\cdots PLP\cdots$ should lead to the collapse of the basic structure.

The reduction process of $LaBaCuCoO_{5\cdot 2}$ constitutes an example of topochemical reaction as those described for many solid-state decomposition reactions[22] and, in particular, the reduction of ABO_3 related perovskites.[23] Interesting examples are $CaMnO_3$[24] and $LaNiO_3$.[25–27] Both compounds can be reduced to an oxygen stoichiometry of 2.5 atoms per unit formula, while intermediate compositions can be stabilised, under the accurate control of the oxygen content. In the first case, $CaMnO_3$ reduction takes place through the octahedral environments to square pyramids, giving rise to superlattices based on interconnected $[MnO_6]$ octahedra and $[MnO_5]$ square pyramids, usually rotated in the (100) plane. Similar phases are obtained in the La-Cu-O system.[28] Reduction of $LaNiO_3$ involves the formation of square planes which intergrow with the octahedra along the [110] direction. On the other hand, the already discussed reduction process of $YBa_2Cu_3O_7$[17] to $YBa_2Cu_3O_6$[18] is also a topochemical process that involves the change $S_P \rightarrow L$.

Another interesting point is the effect of La/Y substitution. For the same cationic stoichiometry, the La sample ($LaBaCuCoO_{5.2}$) shows higher oxygen content that the corresponding Y sample ($YBaCuCoO_5$).[14] This fact can be understood taking into account the inductive effect on the basis of the different polarizing power, q/r, of La and Y cations. Since this ratio is lower for La,[17] this cation tends to share electrons with the most electronegative element, that is, oxygen. If an excess of negative charge is placed on this element, higher oxidation states are expected for the B (Cu/Co) cation and, therefore, an increase of the oxygen content occurs. The different oxygen content is reflected in the structure. In this sense, $YBaCuCoO_5$ is built up from square pyramids that share corners, and is isostructural with the $YBaCuFeO_5$,[6] while $LaBaCuCoO_{5.2}$ incorporates a $\cdots PO_hP\cdots$ block.

Neither of the synthesised samples shows cationic order. This should be favoured by changing the cation ratio. In fact, the related $Y_2Ba_3Cu_3Co_2O_{12}$ compound[29] has been described as a fivefold perovskite superstructure due to the ordered intergrowth of $YBa_2(Cu,Co)_3O_7$ and $YBa(Co,Cu)_2O_5$ units. In this sense, different compositions in the La-Ba-Cu-Co-O system are under investigation and will due reported in due course.

  0947-6539/02/0824-5699 $ 20.00+.50/0

Experimental Section

A sample of nominal composition $LaBaCuCoO_y$ was prepared from the stoichiometric amounts of $BaCO_3$, La_2O_3, Co_3O_4 and CuO. This mixture was ground in an agate mortar and heated, after carbonate decomposition, at 960 °C during a week with intermediate milling.

The cationic composition was determined by energy-dispersive X-ray spectroscopy (EDS) by using a field emission electron microscope (FEG) Philips CM200 equipped with an EDAX microanalytical system. Powder X-ray diffraction (XRD) was performed using a Philips X'Pert diffractometer with $Cu_{K\alpha}$ radiation. The diffraction data were analysed by the Rietveld method[9] by using the Fullprof program.[10] Selected electron diffraction area (SAED) and high resolution electron microscopy (HREM) studies were carried out on both JEOL 2000-FX and JEOL 4000-EX electron microscopes. Oxygen content was determined by thermogravimetric analysis by using a Cahn D-200 electrobalance equipped with a furnace and a two-channel register, allowing simultaneously recording of the weight loss and the reaction temperature. The oxygen content can be determined within $\pm 5 \times 10^{-3}$ for a sample of total mass of about 50 mg.

According to EDS and thermogravimetric analysis, the stoichiometry of the sample was $LaBaCuCoO_{5.2}$. However, it is worth emphasizing that EDS analysis indicates that, although in average constant, the Cu/Co ratio changed over small areas. Reduced samples of general formula $LaBaCuCoO_{5.2-\delta}$ were prepared by reduction of the starting material at 350 °C in an H_2/He atmosphere. Once a desired weight loss, monitored with a CAHN-D200 electrobalance, was attained, the sample was annealed at 700 °C under He atmosphere. δ values were chosen according to the reduction path described in the text.

Acknowledgements

Financial support through research project MAT2001 – 1440 (Spain) is acknowledged.

[1] G. Thornton, B. C. Tofield, A. W. Hewat, *J. Solid State Chem.* **1986**, *61*, 301 – 307.
[2] Y. H. Taguchi, Y. Takeda, F. Kanamaru, M. Shimada, M. Koizumi, *Acta Crystallogr. Sect. B* **1977**, *33*, 1298 – 1299.
[3] A. Maignan, C. Martin, D. Pelloquin, N. Nguyen, B. Raveau, *J. Solid State Chem.* **1999**, *142*, 247 – 260.
[4] C. Martin, A. Maignan, D. Pelloquin, N. Nguyen, B. Raveau, *Appl. Phys. Lett.* **1997**, *71*, 1421 – 1423.
[5] P. E. Schiffer, A. P. Ramírez, W. Bao, S. W. Cheong, *Phys. Rev. Lett.* **1995**, *75*, 3336 – 3339.
[6] L. Er-Rakho, C. Michel, Ph. Lacorre, B. Raveau, *J. Solid State Chem.* **1988**, *73*, 531 – 535.
[7] L. Barbey, N. Nguyen, V. Caignaert, F. Studer, B. Raveau, *J. Solid State Chem.* **1994**, *112*, 148 – 156.
[8] F. Menil, *J. Phys. Chem. Solids.* **1985**, *46*, 763 – 789.
[9] H. V. Rietveld, *J. Appl. Crystallogr.* **1969**, *2*, 65 – 71.
[10] J. Rodríguez-Carvajal, *J. Physi*ca. **1993**, *B192*, 55 – 69.
[11] A. Vegas, M. Vallet-Regí, J. M. González-Calbet, M. A. Franco, *Acta Crystallogr. Sect. B* **1986**, *42*, 167 – 172.
[12] M. A. Alario-Franco, J. M. González-Calbet, M. Vallet-Regí, *J. Solid State Chem.* **1986**, *65*, 383 – 391.
[13] Q. Huang, P. Karen, V. L. Karen, A. Kjekhus, J. W. Lynn, A. D. Mighell, N. Rosov, A. Santoro, *Phys. Rev. B* **1992**, *45*, 9611 – 9619.
[14] S. Howmöller, *Ultramicroscopy* **1992**, *40*, 121 – 135.
[15] P. V. Vanitha, A. Arulraj, P. N. Santhosh, C. N. R. Rao, *Chem. Mater.* **2000**, *12*, 1666 – 1670.
[16] L. Barbey, N. Nguyen, V. Caignaert, M. Hervieu, B. Raveau, *Mater. Res. Bull.* **1992**, *27*, 295 – 301.
[17] M. K. Wu, J. R. Ashburn, C. J. Torng, P. H. Hor, R. L. Meng, L. Gao, Z. J. Huang, Y. Q. Wang, C. W. Chu, *Phys. Rev. Lett.* **1987**, *58*, 908 – 910.
[18] J. B. Parise, E. E. McCarron, *J. Solid State Chem.* **1989**, *83*, 188 – 197.
[19] R. D. Shannon, *Acta Crystallogr. Sect. A* **1976**, *32*, 751 – 767.
[20] C. N. R. Rao, J. M. Thomas, *Acc. Chem. Res.* **1985**, *18*, 113 – 119.
[21] T. Siegriest, S. Zahurak, D. W. Murphy, R. S. Roth, *Nature* **1988**, *334*, 231 – 232.
[22] C. N. R. Rao, B. Raveau in *Transition Metal Oxides*, Wiley, New York **1998**, p. 335.
[23] B. G. Hyde, Sten Andersson in *Inorganic crystal structures*, *Topological Transformation*, Wiley, New York **1988**, p. 295.
[24] A. Reller, J. M. Thomas, F. R. S., D. A. Jefferson, M. K Uppal, *Proc. R. Soc. London Ser. A* **1984**, *394*, 223 – 241.
[25] K. Vidyasagar, J. Gopalakrishnan, C. N. R. Rao, *J. Chem. Soc. Chem. Commun.* **1985**, 7 – 8.
[26] C. N. R. Rao, J. Gopalakrishnan, K. Vidyasagar, A. K. Gangulli, A. Ramanan and L. Ganapathi, *J. Mater. Res.* **1986**, *1*, 280 – 294.
[27] J. M. González-Calbet, M. J. Sayagués, M. Vallet-Regí, *Solid State Ionics* **1989**, *32/33*, 721 – 726.
[28] J. F. Bringley, B. A. Scott, S. J. Laplaca, N. F. Booehme, T. M. Shaw, W. W. McElfresh, S. S. Trail, D. E. Cox, *Nature* **1990**, *347*, 263 – 265.
[29] W. Zhou, D. A. Jefferson, *J. Solid State Chem.* **1995**, *115*, 407 – 410.

Received: August 5, 2002 [F4319]

